

Genomic Structural Equation Modeling Reveals Latent Phenotypes in the Human Cortex with Distinct Genetic Architecture

Rajendra A. Morey MD ^{1, 2, 3}, Yuanchao Zheng MS ^{4, 5}, Delin Sun PhD ^{1, 2}, Melanie E. Garrett MS ^{1, 6}, Marianna Gasperi PhD ⁷⁻⁹, Adam X. Maihofer PhD ^{8, 9}, Lexi Baird BS ², Katrina L. Grasby PhD ¹², Ashley Huggins PhD ^{1, 2, 3}, Courtney C. Haswell MS ^{1, 2}, C. Paul M. Thompson PhD ¹⁰, Sarah Medland PhD ¹¹, Daniel E. Gustavson PhD ¹³⁻¹⁵, Matthew S. Panizzon PhD ¹⁶, William S. Kremen ¹⁶, Caroline M. Nievergelt, PhD ⁷⁻⁹, Allison E. Ashley-Koch PhD ^{1, 6}, Mark W. Logue PhD ^{4, 5, 17, 18}

¹ Brain Imaging and Analysis Center, Duke University, Durham, NC, USA.

40 Medicine Circle Drive

Durham NC 27710

² Department of Psychiatry and Behavioral Sciences, Duke University School of Medicine, Durham, NC, USA.

³ VISN 6 MIRECC, Durham VA Health Care System, Durham, NC, USA.

3022 Croasdale Drive, Suite 300

Durham NC 27705, USA

⁴ National Center for PTSD
VA Boston Healthcare System
150 South Huntington Ave
Boston MA 02130

⁵ Department of Biostatistics,
Boston University School of Public Health
Crosstown Building
801 Massachusetts Avenue 3rd Floor
Boston, MA 02118

⁶ Department of Medicine, Duke Molecular Physiology Institute,
Carmichael Building
300 North Duke Street
Duke University Medical Center,
Durham, NC 27701, USA.

⁷ VA Center of Excellence for Stress and Mental Health,
VA San Diego Healthcare System
3350 La Jolla Village Dr
San Diego, CA 92161 USA

⁸ Research Service
VA San Diego Healthcare System
3350 La Jolla Village Dr
San Diego, CA 92161 USA

⁹ Department of Psychiatry
University of California San Diego
9500 Gilman Drive
La Jolla, CA 92093, USA

¹⁰ Imaging Genetics Center, Stevens Neuroimaging & Informatics Institute
Keck School of Medicine
University of Southern California
2025 Zonal Avenue
Los Angeles, CA 90033, USA.

¹¹ Queensland Institute for Medical Research,
Berghofer Medical Research Institute,
300 Herston Road, Herston
Queensland 4006
Brisbane, QLD, Australia

¹² Psychiatric Genetics, QIMR Berghofer Medical Research Institute, Brisbane, QLD, Australia.
Berghofer Medical Research Institute,
300 Herston Road, Herston
Queensland 4006
Brisbane, QLD, Australia

¹³ Institute for Behavior Genetics
University of Colorado Boulder
1480 30th St
Boulder, CO 80303, USA

¹⁴ Center for Behavior Genetics of Aging
University of California San Diego
9500 Gilman Drive
La Jolla, CA 92093, USA

¹⁵ Department of Psychiatry
Boston University School of Medicine,
720 Harrison Avenue
Boston, MA 02118

¹⁶ Biomedical Genetics,
Boston University School of Medicine,

72 East Concord Street, E200
Boston, MA 02118-2526

Corresponding Author:

Rajendra A. Morey MD

Associate Professor of Psychiatry and Behavioral Sciences, Faculty Member of the Duke Institute for Brain Sciences, Member of the Center for Brain Imaging and Analysis
VISN 6 MIRECC, Durham VA Health Care System, Durham, NC, USA.

3022 Croasdaile Drive, Suite 300

Durham NC 27705, USA

Phone: 857-364-4079

Email: rajendra.morey@duke.edu

Keywords:

Genetically Informed Brain Networks, Genomic Structural Equation Modeling (gSEM), Cortex, Cortical Thickness, Cortical Surface Area, Genome Wide Association Study (GWAS), pleiotropy, structural covariance networks (SCN).

HIGHLIGHTS

- Genomic SEM can examine genetic correlation across cortical regions.
- We inferred regional genetic networks of cortical thickness and surface area.
- Network-associated variants have been implicated in multiple traits.
- These networks are genetically correlated with several psychiatric disorders including MDD, bipolar, ADHD, and alcohol dependence.

ABSTRACT

Genetic contributions to human cortical structure manifest pervasive pleiotropy. This pleiotropy may be harnessed to identify unique genetically-informed parcellations of the cortex that are neurobiologically distinct from anatomical, functional, cytoarchitectural, or other cortical parcellation schemes. We investigated genetic pleiotropy by applying genomic structural equation modeling (SEM) to model the genetic architecture of cortical surface area (SA) and cortical thickness (CT) of 34 brain regions recently reported in the ENIGMA cortical GWAS. Genomic SEM uses the empirical genetic covariance estimated from GWAS summary statistics with LD score regression (LDSC) to discover factors underlying genetic covariance. Genomic SEM can fit a multivariate GWAS from summary statistics, which can subsequently be used for LD score regression (LDSC). We found the best-fitting model of cortical SA was explained by 6 latent factors and CT was explained by 4 latent factors. The multivariate GWAS of these latent factors identified 74 genome-wide significant (GWS) loci ($p < 5 \times 10^{-8}$), including many previously implicated in neuroimaging phenotypes, behavioral traits, and psychiatric conditions. LDSC of latent factor GWAS results found that SA-derived factors had a positive genetic correlation with bipolar disorder (BPD), and major depressive disorder (MDD), and a negative genetic correlation with attention deficit hyperactivity disorder (ADHD), MDD, and insomnia, while CT factors displayed a negative genetic correlation with alcohol dependence. Jointly modeling the genetic architecture of complex traits and investigating multivariate genetic links across phenotypes offers a new vantage point for mapping genetically informed cortical networks.

1. INTRODUCTION

A number of different neurobiological markers have been employed in conjunction with various organizational schemes to map the human cortex. It is possible that individual differences in regional cortical surface area (SA) and cortical thickness (CT) and may drive factors that affect each person and each region independently. However, the covariance structure of regional SA and CT reveals that individual differences are systematically coordinated within communities of brain regions, fluctuate in magnitude together within a population, may be instantiated as structural covariance networks (SCN)¹, and partially recapitulate established organizational schemes²⁻⁵. For instance, SCN organization is consistent with topological patterns of cortical maturation observed throughout developmental stages from childhood and adolescence into early adulthood⁶, and the same patterns are then targeted by neurodegenerative diseases in late life^{7,8}. Second, brain regions with highly correlated CT or SA often represent networks that perform dedicated cognitive processes^{1,9,10}. Third, regions within SCNs tend to be directly connected by white matter tracts. Indeed, about 40% of SCN connections show convergent white matter fiber connections, although other relationships captured by SCNs are independent of fiber connectivity⁵.

The correlation structure between regions represented by an SCN is influenced by both the environment and genetics. The genetic factors underlying structural correlations closely resemble functional and developmental patterns^{4,5,11}. We will refer to these patterns of genetic correlations between brain regions as *genetically informed brain networks* (GIBNs). Genetic correlations of CT or SA have been examined with twin studies^{12,13}. These genetic influences were recapitulated in over 400 twin pairs, to show that the cortex is organized genetically into communities of structural and functional regions, is hierarchical, is modular, and is bilaterally symmetric¹¹. Their genetically informed parcellation identified 12 spatially contiguous regions that qualify as GIBNs. Relatedly, SA and CT phenotypes overlap genetically with GIBNs, the latter being less granular and more discoverable¹⁴.

While twin studies have laid important groundwork regarding genetic correlations of the brain, they have several limitations. First, twin studies do not provide specific genetic variants

associated with each GIBN¹¹ and therefore offer an incomplete characterization of cortical pleiotropy. Second, twin studies rely on the *equal environment* assumption, which may be invalid for some studies. Third, quantifying the genetic correlation between GIBNs and low prevalence traits such as schizophrenia (0.5% prevalence)¹⁵ or bipolar disorder (1% prevalence)¹⁶ would require an extraordinarily large number of twin pairs to wield sufficient statistical power. Recently, genetic correlations between brain regions derived from GWAS results have been applied to estimate the contribution of common genetic variation. This method confers several advantages over twin studies. These SA and CT GWAS results reveal pleiotropy and genetic correlation across many neuroimaging phenotypes^{17,18}. Additionally, genome-wide SNP data allow effect-size estimation for individual variants and the ability to test genetic correlations with other traits in different populations.

Genomic structural equation modeling (gSEM) is a multivariate statistical method that leverages the genetic architecture of many genetically correlated phenotypes to derive relatively few latent phenotypes, which explain the observed genetic correlation and loadings of multiple phenotypes onto a latent phenotype¹⁹. Therefore, gSEM applied to GWAS offers a genetically informed parcellation of the cortex that is neurobiologically distinct from anatomical, functional, cytoarchitectural, and other parcellation schemes^{6,20}. Latent factors represent traits that explain the genetic correlation across multiple regions and define the brain regions that constitute each GIBN. Importantly, gSEM estimates the strength of association between genetic variants and each latent factor followed by a multivariate GWAS of each GIBN using GWAS summary statistics for individual correlated traits. Importantly, gSEM provides a description of the underlying genetic architecture of the traits being examined and effect size estimates for the underlying latent factors.

In the present study, we sought to elucidate the genetic architecture of 34 regional SA and CT phenotypes reported in the ENIGMA-3 GWAS of over 50,000 primarily healthy individuals. We hypothesized that gSEM might identify brain partitions consistent with the 12 clusters described by Chen et al.¹¹, along with other viable solutions. The genetic correlations reported in Grasby et al.¹⁸, were stronger within major anatomical lobes than across lobes. Thus, while we predicted gross lobar structure may be reflected by GIBNs, we further predicted that GIBNs

would reflect the complex relationships captured by functional networks, canonical resting-state networks, fiber tract networks, gene expression networks, and other neurobiological systems^{6,11}. We hypothesized from the outset that most genetic variants discovered by the ENIGMA-3 cortical GWAS would influence GIBNs in the present study, but we also sought to discover novel genetic markers, and discover links between known genetic variants and established regional associations as well as GIBNs. Additionally, we hypothesized genetic correlations between GIBNs and major neuropsychiatric disorders.

2. METHODS

2.1 Data

We used the results of the ENIGMA-3 cortical GWAS that identified genetic loci associated with variation in cortical SA and CT measures in 51,665 individuals primarily (~94%) of European descent, from 60 international cohorts¹⁸. Phenotype measures were extracted from structural MRI scans for 34 regions defined by the Desikan-Killiany atlas using gyral anatomy, which establishes coarse partitions of the cortex²¹. Two global measures of total cortical SA and average CT, as well as 34 regional measures of SA and CT were averaged across left and right hemisphere structures to yield 70 distinct phenotypes. Multiple testing correction in the ENIGMA-3 GWAS was based on 60 independent phenotypes with a GWS threshold of $P \leq 8.3 \times 10^{-10}$. We accessed the GWAS summary results for the 34-regional bilateral analyses performed by Grasby et al. The primary GWAS presented in Grasby et al. had adjusted for global measures (total SA and mean CT). However, we requested alternate results without global adjustments to avoid artefactual negative (inverse) correlations between regions. Regional SA and CT metrics were analyzed separately.

2.2 Analysis

Our analyses were performed using the genomic-SEM package which is available for the R programming language¹⁹. The entire gSEM was performed twice, once for 34 SA regions and

once for 34 CT regions. Like standard SEM, gSEM includes an exploratory factor analysis (EFA) stage and a confirmatory factor analysis (CFA) stage. To avoid overfitting between the confirmatory and exploratory phases, we analyzed odd chromosomes in the EFA and even chromosomes in the CFA. Whereas SEM often fits multiple models corresponding to *a priori* hypotheses built on theoretical models, we took a hypothesis free (data driven) approach. In the EFA, we fit one model, which included up to 10 factors, for each of SA and CT. The optimal number of factors for each was determined using scree plots (see Supplementary **Figures S1** and **S2**). Positive factor loading estimates greater than a pre-specified threshold were carried forward to the confirmatory factor model stage to be re-estimated, and the remaining loading parameters were set to zero. As there was no consensus on factor loading cutoffs ^{22,23}, we tested thresholds 0.3 and 0.5. Cross loadings that were allowed if they exceeded the threshold. Factors that loaded on only a single region were removed from CFA modeling. Therefore, some models with a large number of factors ended up as redundant, and were not carried forward to CFA.

All of the distinct factor structures generated were carried forward to CFA and re-estimated using even chromosomes. Standardized root-mean square residual (SRMR), Akaike Information Criteria (AIC), model χ^2 , and Comparative Fit Index (CFI) were used to evaluate model fit of the CFA models. The large number of GWASs and the large sample size of each GWAS meant that all model χ^2 statistics were highly significant ($p \sim 0$) and hence are not presented.

The top performing factor models in the CFA were further optimized by successive removal of non-significant factor loadings. In addition, we attempted to fit a bifactor model as part of the CFA step to account for correlation between the factors. Specifically, we fit a bifactor model where a “total” CT or SA factor was added, which loaded on all regions, and a multi-level model where all factors from the EFA loaded onto a 2nd order factor. The bifactor model failed to converge for all CFA models and the multilevel model failed to improve model fit; hence these results are not presented. For our purposes, a model which minimized the AIC was deemed optimal. SRMR and CFI were calculated to measure model fit.

Once the GIBNs were defined, we used gSEM to generate a multivariate GWAS of each GIBN. The GWS associations ($p < 5 \times 10^{-8}$) for each GIBN were compared to the significant SNPs reported by Grasby et al. (with global correction) and then compared to the corresponding GWAS results without the global correction (the same results used to generate GIBNs). The *FUnctional M*apping and *A*nnnotations (FUMA) package²⁴ was used to annotate results from each GIBN GWAS, including annotating SNPs to specific genes, and identifying potential functional variants. FUMA was run based on LD in the 1000G Phase3 EUR reference panel²⁵ and the default FUMA parameter settings.

2.3 Polygenicity Analysis

We examined the significant SNPs from the GIBN GWAS, as well as SNPs in LD using FUMA to test for functional associations with established behavioral traits and major neuropsychiatric disorders. First, we examined whether observed variants from the GWAS recapitulated GWS SNPs from previous GWAS results of neuroimaging traits including cortical GWAS results and other structural neuroimaging parameters^{17,26-31}. We also looked for SNPs that were significant in GWASs of 12 neuropsychiatric disorders from the Psychiatric Genomics Consortium (PGC): ADHD³², alcohol dependence³³, anorexia nervosa³⁴, autism spectrum disorder³⁵, bipolar³⁶, cannabis use³⁷, MDD³⁸, obsessive compulsive disorder (OCD)³⁹ posttraumatic stress disorder (PTSD)⁴⁰, schizophrenia⁴¹, Tourette's syndrome⁴², and anxiety⁴³. Finally, FUMA was used to functionally annotate loci that overlapped with previously published GWAS results.

Genetic Correlation with Psychopathology

We used cross-trait LDSC to identify links between psychiatric disorders and CT-derived GIBNs as well as psychiatric disorders and SA-derived GIBNs⁴⁴. We estimated the genetic correlation between CT- and SA-derived GIBNs and neuropsychiatric disorders using their GWAS summary statistics⁴⁴. To maximize statistical power, we limited the number of genetic correlations to 12 neuropsychiatric disorders.

2.4 Data and Code Availability

The GWAS summary statistics which were used in this paper are available to download from the ENIGMA consortium website (<http://enigma.ini.usc.edu/research/download-enigma-gwas-results>). Access to cohort data is available either through public repositories or directly from the cohort. Direct requests are required when informed consent or the approved study protocol does not permit deposition into a repository. Requests for data by qualified investigators are subject to scientific and ethical review to ensure that the data will be used for valid scientific research and to ensure compliance with confidentiality, consent, and data protection regulations. Some of the data are subject to material transfer agreements or data transfer agreements, and specific details on how to access data for each cohort are available in Grasby et al (2020). The Genomic SEM package used to analyze the data is publicly available at <https://github.com/GenomicSEM/GenomicSEM>. The ldsc package is publically available at <https://github.com/bulik/ldsc>. The results of the multivariate GWASs of the CT- and SA-derived GIBNs are available at <https://pgc-ptsd.com/about/workgroups/imaging-workgroup/>.

3. RESULTS

3.1 Model Fit

The SA-derived 6-GIBN solution resulted in the best overall model fit to the genetic covariances generated from the GWAS summary statistics (AIC=22,712,604, CFI=0.920, SRMR=0.062). See Supplementary **Table S1** for fit statistics for each evaluated model. The 6 SA-derived GIBNs (SA1-SA6) loaded on 24 of the 34 brain regions¹⁸. The standardized estimates for the 6 SA-derived GIBN models (standardized factor loadings) are presented in Supplementary **Table S2** and presented in **Figure 1**. The GIBNs generally encompass contiguous brain regions and many correspond to known neuroanatomical features. SA1 contains loadings for inferior temporal, isthmus cingulate, postcentral, precuneus, superior parietal, supramarginal, and temporal pole. SA2 contains loadings for caudal anterior cingulate, caudal middle frontal, medial orbitofrontal, paracentral, and rostral anterior cingulate. SA3 contains loadings for banks superior temporal sulcus (STS), inferior parietal, and middle

temporal. SA4 contains loadings for pars opercularis, pars orbitalis, and pars triangularis, SA5 contains loadings for cuneus, lateral occipital, lingual, and pericalcarine, and SA6 corresponds to the auditory cortex. The 6-factor model indicated substantial correlation between GIBNs ($r_g=0.61$ to 0.91) as reported in Supplementary **Table S3**.

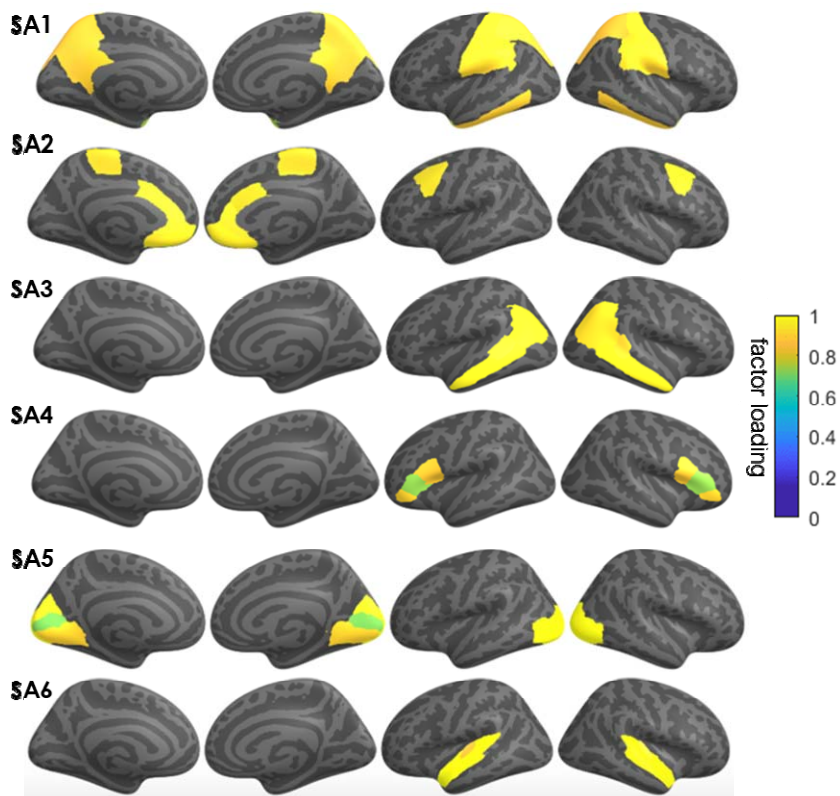


Figure 1. Genomic structural equation modeling (gSEM) jointly modeled the genetic architecture of cortical surface area (SA) for 34 brain regions based on GWAS results of Grasby et al (2020). The model generated 6 genetically informed brain networks (GIBNs) from SA phenotype measures. The color overlay on cortical regions represents the magnitude of the factor loadings indicated in the color gradient (yellow = high; blue = low). Subsequent GWAS identified several genome wide significant hits ($p < 5 \times 10^{-8}$) associated with each GIBN.

The CT-derived 4-GIBN solution resulted in the best model fit ($AIC=17761928$, $CFI=0.932$, $SRMR=0.077$; Supplementary **Table S4**). Significant non-zero loadings for CT-derived GIBNs loaded on 25 of the 34 brain regions from Grasby et al. See Supplementary **Table S5** for the estimated loadings that are visualized in **Figure 2**. As observed with SA models, the CT-derived GIBNs generally encompassed contiguous cortical regions. CT1 contains loadings for banks STS, caudal middle frontal, inferior parietal, paracentral, pars opercularis, post-central,

pre-central, precuneus, rostral middle frontal, superior frontal, superior parietal, and supramarginal cortices. CT2 contains loadings for caudal anterior cingulate, frontal pole, insula, lateral orbitofrontal, medial orbitofrontal, pars orbitalis, rostral anterior cingulate, and rostral middle frontal. CT3 contains loadings for banks STS, superior temporal, and temporal pole. CT4 contains loadings for cuneus, lateral occipital, parahippocampal, and pericalcarine cortices. The CT-derived GIBNs were moderately to highly correlated ($r_g=0.67$ to 0.87 ;

Supplementary Table S6).

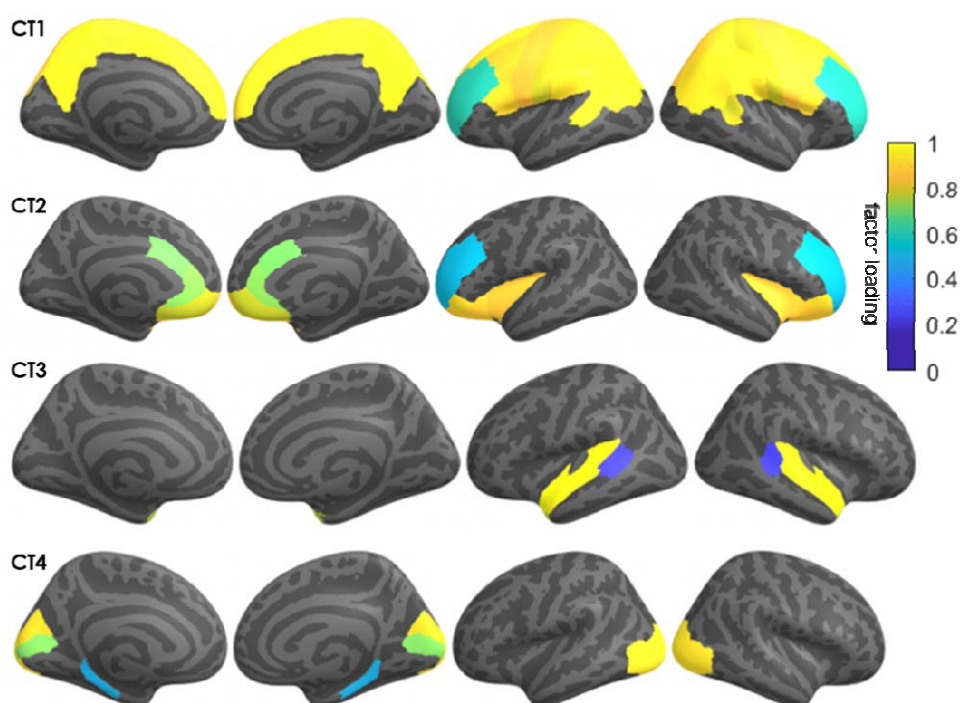


Figure 2. Genomic structural equation modeling jointly modeled the genetic architecture of cortical thickness (CT) for 34 brain regions based on GWAS results of Grasby et al (2020). The model generated 4 genetically informed brain networks (GIBNs) from CT phenotype measures. The color overlay on cortical regions represents the magnitude of the factor loadings indicated in the color gradient (yellow = high; blue = low). Subsequent GWAS identified several genome wide significant hits ($p < 5 \times 10^{-8}$) associated with each GIBN.

Factor diagrams for SA- and CT-derived GIBNs are presented in **Figure 3**. Consistent with prior work, the SA-derived GIBNs were largely distinct from CT-derived GIBNs, although some regional overlap exists between SA- and CT-derived GIBNs. For example, SA5 and CT4 are both 4-region GIBNs, with 3 overlapping regions.

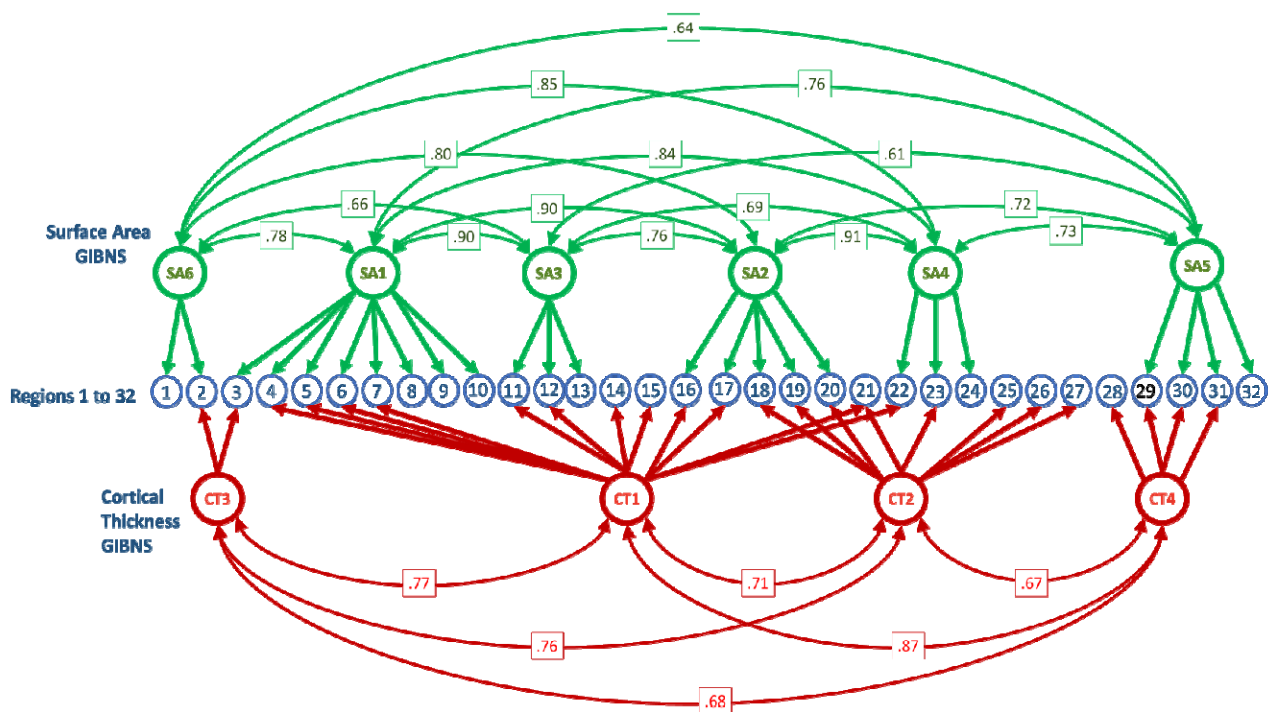


Figure 3. Graph of generic structural equation modeling (gSEM) results. The blue circles, numbered from 1 to 32, represent the cortical surface area (SA) and cortical thickness (CT) of regions defined by the Desikan-Killany atlas. Latent SA variables, indicated by green circles, represent the genetic contributions from regional SA, which are specified by thick green lines and arrows. Latent CT variables, indicated by red circles, represent the genetic contributions from regional CT, which are specified by thick red lines and arrows. Thin green lines connect genetically latent SA variables with their genetic correlation strength (r_g) indicated in green boxes. Thin red lines connect genetically latent CT variables with their genetic correlation strength (r_g) indicated in red boxes.

3.2 GWAS of Genetically Informed Brain Networks

To identify specific genetic variants that may be influencing the GIBNs, we performed a multivariate GWAS on each SA- and CT-derived GIBN. Manhattan plots for SA- and CT-derived GIBN GWASs, their associated quantile-quantile (QQ) plots, and genomic inflation factors (λ) are provided in **Figures S3 to S12**. We observed moderate p-value inflation (λ values between 1.06 and 1.16). However, the single-trait LD Score regression intercepts for SA- and CT-derived GIBNs were all less than 1.02, indicating that the apparent inflation was likely due to pleiotropy. A total of 5,843 GWS ($p < 5 \times 10^{-8}$) variants were associated with 10 GIBNs. Annotation by FUMA²⁴ mapped these variants to 74 independent regions, including 64 loci that were associated with the 6 SA-derived GIBNs and 10 loci that were associated with the 4 CT-derived GIBNs. A phenogram⁴⁵ of the 74 genetic associations is presented in **Figure 4**. A list of all GWS loci with their associated GIBNs is provided in Supplementary **Table S7**. Except for two novel SNPs, all others were previously identified in Grasby et al.¹⁸ in either the analysis adjusted for global SA/CT or the unadjusted analysis. The first novel SNP rs3006933,

which resides near the genes *SDCCAG8* and *AKT3* on chromosome 1, was associated with SA1 ($p=4.08\times 10^{-9}$). The other novel SNP rs1004763 on chromosome 22, which resides in the vicinity of gene *SLC16A8*, was associated with CT2 ($p=3.41\times 10^{-08}$).

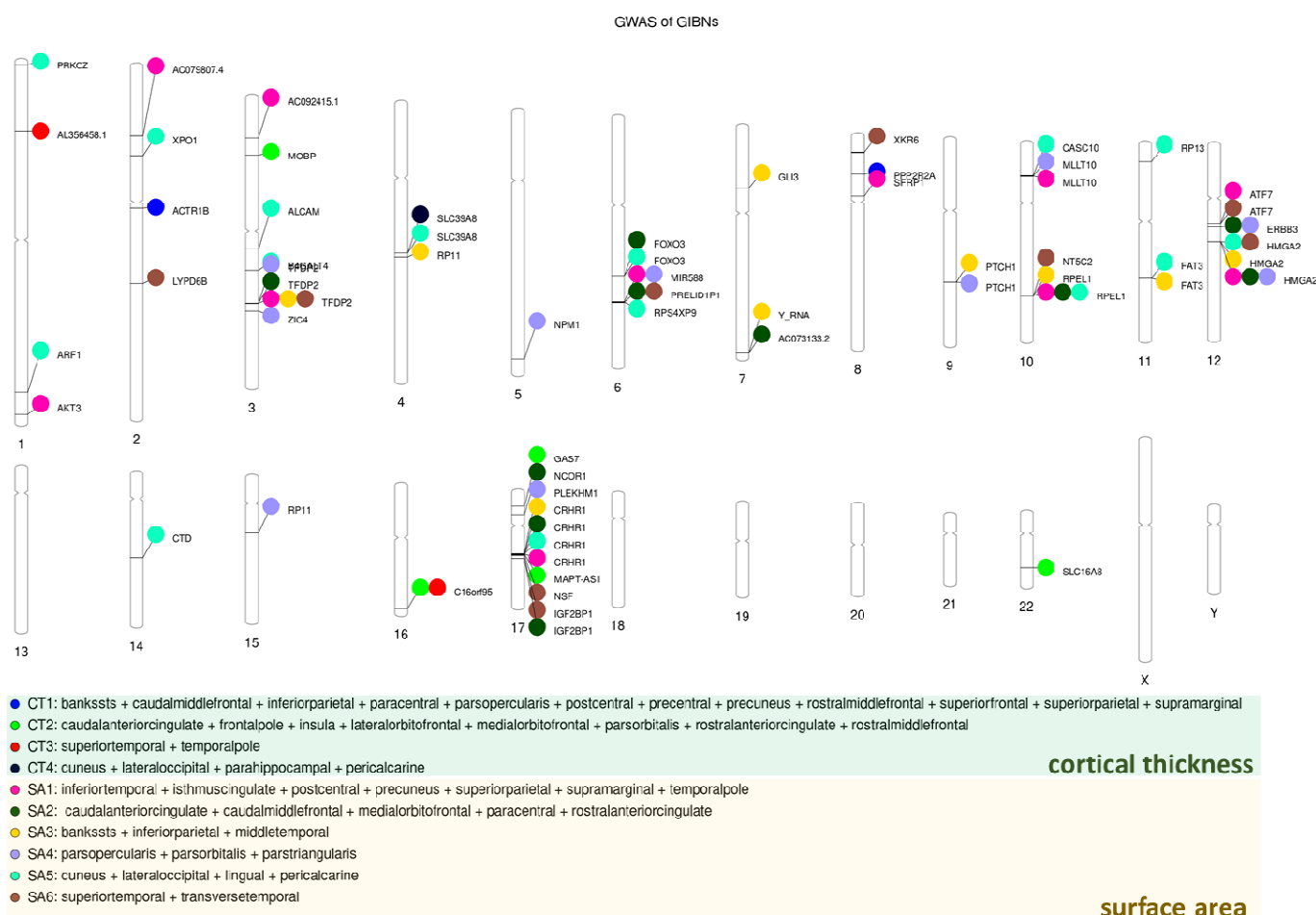


Figure 4. Phenogram of GWS SNPs associated with six genetically informed brain networks (GIBNs) derived from surface area (SA; gold inset) and four GIBNs derived from cortical thickness (CT; green inset).

3.3 Genetic Correlation

We observed significant genetic correlation between multiple traits and SA-derived GIBNs as reported in Supplementary **Table S8**. ADHD exhibited significant negative genetic correlation with all SA-derived GIBNs except SA4 ($r_g=-0.13$ to -0.20 , $p=3.29 \times 10^{-6}$ to 0.0038 , $p_{FDR}=0.00040$ to 0.039). Significant positive genetic correlations were observed between bipolar disorder and SA1, SA2, SA4, and SA5 ($r_g=0.10$ to 0.14 , $p=3.00 \times 10^{-4}$ to 0.0047 , $p_{FDR}=0.012$ to 0.043). Interestingly, we observed significant genetic correlations between MDD and SA-derived GIBNs, but in the opposite direction as bipolar disorder. We found a significant negative

correlation between MDD and SA6, which was not associated with bipolar disorder ($r_g=-0.10$, $p=0.0011$, $p_{FDR}=0.17$). Negative nominally significant (uncorrected $p<0.05$) correlations were observed between MDD SA1-SA3, and SA5 ($r_g= -0.057$ to -0.080 , $p=0.0090$ to 0.046), while SA4 was not genetically correlated with MDD ($p=0.12$). SA4 was significantly correlated with cannabis use disorder ($r_g=0.15$; $p=4.00 \times 10^{-4}$, $p_{FDR}=0.012$), while SA2 was nominally associated with cannabis use ($r_g=0.11$, $p=0.011$). No significant genetic correlations were observed between the 6 SA-derived or 4-CT derived GIBNs and anorexia, autism, anxiety, schizophrenia, PTSD, or Tourette's Syndrome (all $p>0.05$).

Fewer genetic correlations were significant between CT-derived GIBN regions and psychiatric disorders (Supplementary **Table S9**). CT3 and CT4 were negatively correlated with alcohol use disorder, exhibiting the strongest correlations with any traits that we examined (CT3 $r_g=-0.35$, $p=3 \times 10^{-4}$, $p_{FDR}=0.012$; CT4 $r_g=-0.31$, $p=7 \times 10^{-4}$, $p_{FDR}=0.014$). We found a negative nominally significant correlation between alcohol use disorder and CT1 ($r_g=-0.18$, $p=0.035$, $p_{FDR}=0.22$). CT3 had a positive nominally significant correlation with OCD ($r_g=0.22$, $p=0.0091$, $p_{FDR}=0.078$).

The overlap of the GIBN GWS loci with prior GWAS of neuroimaging phenotypes or psychiatric disorders firmly points to the relevance of GIBN-related variants to brain structure and cognition. First, we note that novel variant rs3006933 has been previously associated with subcortical volumes⁴⁶. Novel variants rs3006933 and rs1004763^{17,29} have been associated with neuroimaging phenotypes of corpus callosum white matter microstructure⁴⁷. A comparison of our GIBN GWAS with published psychiatric disorder GWAS results found that multiple SNPs linked to SA-derived GIBNs were also implicated in a GWAS of schizophrenia⁴¹. Specifically, we identified a cluster of 4 loci in the *CRHR1* gene strongly associated with SA-derived GIBNs (rs62057153 associated with SA1) in our GWAS ($p=5.22 \times 10^{-17}$ to 8.45×10^{-21}). We also observed an association between CT1 and rs11692435 ($p=1.17 \times 10^{-12}$), a schizophrenia-related locus, within the *ACTR1B* gene. Finally, CT- and SA-derived GIBNs were associated with schizophrenia risk variants in the *SLC39A8* gene; namely rs13107325 was associated with CT5 and rs13135092 was associated with SA5. No other traits had GWS variants associated with any of the GIBNs.

Annotation of GIBN-related SNPs using FUMA found that many have been previously associated with cognitive, behavioral, neuroanatomical, neurofunctional, and neuropsychiatric phenotypes. In addition to rs3006933 noted above¹⁴, SA6-linked locus rs9909861⁴⁸ and SA5-linked SNP rs7570830¹⁴ have also been associated with subcortical volumes. Multiple loci associated with SA-derived GIBNs that encompass temporal, parietal, and temporo-parietal association cortices include SA1-linked locus rs10109434⁴⁹, SA3-linked SNP rs2299148⁵⁰, and SA6-linked locus rs9909861⁵⁰⁻⁵⁴ have previously been implicated in academic attainment and cognitive ability. These GIBNS, particularly temporal (SA6) and temporoparietal (SA3) cortices, are the most more strongly linked to academic attainment and the most heritable⁵⁵. The SA5-linked locus rs6701689 has been reported for risk tolerance⁵⁶. However, there is no support for this GIBN in the visual cortex (SA5) plays a role in risk tolerance, which is linked to cerebellar, midbrain, and prefrontal cortical anatomy, as well as glutamatergic and GABAergic neurotransmission^{56,57}. The CT4-associated locus rs13107325 has been associated with many traits including schizophrenia⁵⁸⁻⁶⁵, bipolar disorder^{62,63}, Parkinson's disease^{64,65}, sedentary behavior^{46,66} and risk taking⁵⁶, as well as cognition, intelligence, and educational attainment^{50-54,67}. This GIBN includes the parahippocampal and fusiform gyri, which have a firmly established link to schizophrenia⁶⁸ and a recently identified link to sedentary behavior⁶⁹.

4. DISCUSSION

The goal of the present study was to leverage the pleiotropic architecture of the human cortex to construct a genetically informed parcellation that could be distinct from anatomical, functional, cytoarchitectural, or other established parcellation schemes, although, our analysis starts with a somewhat crude anatomically-based 34-region parcellation. We investigated the genetic pleiotropy of regional cortical morphology by applying gSEM to jointly model the genetic architecture of 34 brain regions using results from the ENIGMA-3 GWAS¹⁸. The process was undertaken with gSEM to generate several possible solutions, from which the best-model fit was selected. This solution organized brain regions to optimally assign genetic pleiotropy to 6 SA- and 4 CT-derived latent factors, which we have termed *genetically informed brain networks* (GIBNs). Subsequent multivariate GWAS of these GIBNs were mapped by FUMA to 74 independent SNPs ($p < 5 \times 10^{-8}$). LDSC results of CT- and SA-derived GIBNs were

positively correlated with OCD and bipolar disorder, but negatively correlated with alcohol use disorder, ADHD, MDD, and insomnia.

We observed 74 GWS markers associated with the SA- and CT-GIBNs. The overlap of the GIBN GWS loci with prior GWAS of neuroimaging phenotypes or psychiatric disorders firmly points to the relevance of GIBN-related variants to brain structure and cognition. First, we note that novel variant rs3006933 has been previously associated with subcortical volumes⁴⁶. Novel variants rs3006933 and rs1004763^{17,29} have been associated with neuroimaging phenotypes of corpus callosum white matter microstructure⁴⁷. A comparison of our GIBN GWAS with published psychiatric disorder GWAS results found that multiple SNPs linked to SA-derived GIBNs were also implicated in a GWAS of schizophrenia⁴¹. Specifically, we identified a cluster of 4 loci in the *CRHR1* gene strongly associated with SA-derived GIBNs (rs62057153 associated with SA1) in our GWAS ($p=5.22\times 10^{-17}$ to 8.45×10^{-21}). We also observed an association between CT1 and rs11692435 ($p=1.17\times 10^{-12}$), a schizophrenia-related locus, within the *ACTR1B* gene. Finally, CT- and SA-derived GIBNs were associated with schizophrenia risk variants in the *SLC39A8* gene; namely rs13107325 was associated with CT5 and rs13135092 was associated with SA5. No other traits had GWS variants associated with any of the GIBNs.

Annotation of GIBN-related SNPs using FUMA found that many have been previously associated with cognitive, behavioral, neuroanatomical, neurofunctional, and neuropsychiatric phenotypes. In addition to rs3006933 noted above¹⁴, SA6-linked locus rs9909861⁴⁸ and SA5-linked SNP rs7570830¹⁴ have also been associated with subcortical volumes. Multiple loci associated with SA-derived GIBNs that encompass temporal, parietal, and temporo-parietal association cortices include SA1-linked locus rs10109434⁴⁹, SA3-linked SNP rs2299148⁵⁰, and SA6-linked locus rs9909861⁵⁰⁻⁵⁴ have previously been implicated in academic attainment and cognitive ability. These GIBNS, particularly temporal (SA6) and tempoparietal (SA3) cortices, are the most more strongly linked to academic attainment and the most heritable⁵⁵. The SA5-linked locus rs6701689 has been reported for risk tolerance⁵⁶. However, there is no support for this GIBN in the visual cortex (SA5) plays a role in risk tolerance, which is linked to cerebellar, midbrain, and prefrontal cortical anatomy, as well as glutamatergic and GABAergic neurotransmission^{56,57}. The CT4-associated locus rs13107325 has been associated with many

traits including schizophrenia⁵⁸⁻⁶⁵, bipolar disorder^{62,63}, Parkinson's disease^{64,65}, sedentary behavior^{46,66} and risk taking⁵⁶, as well as cognition, intelligence, and educational attainment^{50-54,67}. This GIBN includes the parahippocampal and fusiform gyri, which have a firmly established link to schizophrenia⁶⁸ and a recently identified link to sedentary behavior⁶⁹.

The GIBNs we generated can be compared to similar structures generated from twin studies. Using 400 twin pairs, Chen et al. generated twelve genetically-informed clusters from vertex-based surface area measures¹¹. The 12 clusters consisted of (1) motor-premotor cortex, (2) dorsolateral prefrontal cortex, (3) dorsomedial frontal cortex, (4) orbitofrontal cortex, (5) pars opercularis and subcentral region, (6) superior temporal cortex, (7) posterolateral temporal cortex, (8) anteromedial temporal cortex, (9) inferior parietal cortex, (10) superior parietal cortex, (11) precuneus, and (12) occipital cortex. The results of Chen et al.¹¹ constitute the earliest genetically informed parcellation of the brain, which reported heritability estimates and genetic correlations between clusters. The genetically informed clusters are more consistent with classical anatomically-defined sulcal and gyral boundaries, Brodmann definitions, and cytoarchitectural patterns than our GIBNs. Importantly, our GIBNs, better represent functional specializations than the 12 genetically-informed clusters. However, these published twin studies notably lack any information about specific genetic variants. Thus, our study extends the circumscribed results of earlier twin studies by mapping specific genetic variants onto the cortical covariance structure.

The organization of structural covariance networks is partially reflected in other schemes for organizing the human cortex including resting state networks, gene expression networks, white matter networks and other neurobiological brain features. Structural covariance networks (SCN) tend to reflect white matter connections throughout the cerebral cortex, although other information captured by SCNs is independent of fiber connectivity⁵. More recently, the covariance structure of cortical thickness was shown to be correlated with gene transcriptional networks that are organized with similar complex topology on the basis of modularity, small-worldness, and rich-clubness². Whereas network properties such as degree and degree-distribution differed, the cortical areas connected to each other within SCN modules had higher

levels of gene-co-expression than expected by chance alone². Relatedly, gene co-expression networks are also mirrored by canonical resting-state networks⁷⁰. Specifically, 136 consensus genes are differentially co-expressed in 4 resting-state networks including salience, dorsal default mode, visual, and sensorimotor.

It is now firmly established that resting-state functional connectivity from fMRI evinces robust patterns of synchronous activity that intrinsically organize into canonical resting-state networks⁷¹. These resting state networks are typically identified by applying independent component analysis to the functional connectome⁷². We found that SA-derived GIBNs significantly align with several canonical resting-state networks. Most prominent among them is the recapitulation of the visual network by SA5, which is composed of cuneus, lateral occipital, lingual, and pericalcarine cortices⁷³. Twin-based non-linear multidimensional heritability estimates (of multidimensional traits such as brain network architecture) are among the highest for the visual network (left $h^2_m=0.53$; right $h^2_m=0.45$) and auditory network (left $h^2_m=0.44$; right $h^2_m=0.60$)⁷⁴. SA6, which includes superior and transverse temporal cortices, closely recapitulates the auditory cortex. The functional specializations of the human auditory cortex⁷³, which include parts of the lateral prefrontal cortex, Broca's area, and subcentral regions, are needed for human vocalization and language^{75,76}. The dorsal attention network (DAN), which directs voluntary allocation of attention, is concordant with SA1 that is comprised of superior parietal, supramarginal, postcentral, precuneus, isthmus cingulate, and inferior temporal regions. A noteworthy omission from SA1, which is an important feature of the DAN, are the frontal eye fields (FEF)⁷⁷. The most likely explanation is that the FEF is not a distinct region in FreeSurfer parcellation and therefore this phenotype is not well represented in ENIGMA cortical GWAS. The DAN has relatively high twin heritability estimates (left $h^2=0.45$; right $h^2=0.40$)⁷⁴. The default mode network (DMN), which is sometimes partitioned into dorsal and ventral subnetworks⁷⁸, resembles SA2 and SA3 respectively. The caudal anterior cingulate, caudal middle frontal, medial orbitofrontal, paracentral, and rostral anterior cingulate cortices comprise SA2, while banks of STS, inferior parietal, and middle temporal cortices comprise SA3. SA4 represents a partial recapitulation of the central executive network (CEN) with the pars opercularis, pars orbitalis, and pars triangularis, but lacks the temporoparietal structures, which are a core feature of the CEN⁷⁹.

Our results are consistent with evidence that the functional connectome is shaped by genomic constraints^{74,80}. For instance, twin data from the human connectome project (HCP) shows that individual variability in the areal size of 17 canonical functional networks, as defined by Yeo et al.⁷³, reveal marked heritability ($h^2=0.34$ to 0.40). Unimodal sensory networks such as auditory and visual networks are particularly heritable while hetero-modal networks such as the salience network and the central executive network are significantly less heritable⁷⁴. Overall, the parcellation schemes reflect the genetic influences driving cortical areal expansion and represent genetically driven processes in embryological neurodevelopment.

We find that behavioral traits and neuropsychiatric disorders showed distinct genetic correlations with SA-derived GIBNs that differ markedly from correlations with CT-derived GIBNs. Psychiatric disorders that were significantly genetically correlated with SA-derived GIBNs were not correlated with CT-derived GIBNs, and some CT-derived GIBNs were correlated with other psychiatric disorders that were not correlated with SA-derived GIBNs. CT3, which is located in the middle and superior temporal cortices, and CT4, which is located in the visual perceptual cortex, were strongly negatively correlated with alcohol use disorder. This divergent relationship between CT-derived and SA-derived networks is consistent with our findings from the ENIGMA-3 cortical GWAS where a consistent pattern of significant positive and negative correlations between total brain SA and behavioral traits/disorders was found, but average CT correlations with behavioral traits/disorders were non-significant¹⁸. Specifically, the ENIGMA-3 GWAS found that total SA was significantly positively correlated with cognitive function, educational attainment, Parkinson's disease, and anorexia nervosa, but significantly negatively correlated with MDD, ADHD, depressive symptoms, neuroticism, and insomnia. In addition, the SA-derived GIBNs showed distinct genetic relationships to several psychiatric disorders. Several SA-derived GIBNs (SA1, SA2, SA4, SA5) were positively correlated with bipolar disorder, whereas SA-derived GIBNs (SA1, SA2, SA3, SA5, SA6) were negatively correlated with MDD, buttressing prior evidence that MDD and Bipolar are distinct conditions with divergent genetic bases⁷⁸. While the relationship between these SA-derived GIBNs with MDD converge with the findings from the ENIGMA total surface area results, the relationship with bipolar disorder was novel. The GIBNs may provide additional power to detect genetic relationships when the strength of these relationships across cortical regions is heterogenous. Interestingly, although several GIBN-related SNPs we found were associated with

schizophrenia, there were no GIBNs that were significantly correlated with schizophrenia ($r_g = 0.029$ to 0.034 ; all $p > 0.30$).

There is ample evidence that genetic variants that influence SA are distinct from genetic variants that influence CT¹⁸. Genetic variation affecting gene regulation in progenitor cell types, present in fetal development, affects adult cortical SA⁸¹. An increase in proliferative divisions of neural progenitor cells leads to an expansion of the pool of progenitors, resulting in increases in neuronal production and larger cortical SA, which is more prevalent in gyrencephalic species (e.g. humans, primates)⁸². By contrast, loci near genes implicated in cell differentiation, migration, adhesion, and myelination are associated with CT. The present findings suggest a similar distinction holds in case of SA-derived GIBNs compared to CT-derived GIBNs. We hypothesize that the unique genetic correlations of SA-derived GIBNs and CT-derived GIBNs with behavioral traits/disorders may be explained by the distinct developmental functions of their associated genes. Further exploration of the common and distinct relationships of SA-derived and CT-derived GIBNs with neuropsychiatric conditions using Mendelian Randomization and Latent Causal Variable (LCV) analysis may prove useful⁸³.

4.1 *Limitations*

A number of limitations deserve consideration in interpreting the present findings. Our starting point for the gSEM was the GWAS of 34 cortical regions as defined by the Desikan-Killiany atlas. However, using cortical pleiotropy as an organizing schema for parcellation will not strictly adhere to regions defined by anatomical features. A high-resolution GWAS of the cortex would allow more flexibility in defining parcellation boundaries informed by genetic pleiotropy given it is likely that they differ from anatomically defined parcels. Realizing a high-resolution GWAS of the cortex poses a major computational challenge. For instance, a multivariate GWAS of 1,284 cortical vertex locations²⁶ would be extremely time- and cost-prohibitive. Indeed, the present gSEM with just 34 phenotypes required about 2 weeks per chromosome running on the Shared Computing Cluster (SCC) at Boston University.

The GWAS threshold we used to identify significant associations with the 6 SA-derived and 4 CT-derived GIBNs was $p < 5 \times 10^{-8}$, as we hypothesized that many of the associated loci would have been implicated in the prior GWAS, and we wanted to explore the relationship between

GIBN GWAS variants and other traits. This is supported by the fact that the vast majority GIBN-associated SNPs had been noted in other cortical GWASs^{17,18,29}. However, we note that the two novel SNPs identified, the SA1-associated SNP, rs3006933, would survive a strict Bonferroni correction for 10 GIBN GWASs examined ($p=4.08\times10^{-9}$), while the CT2-associated variant, rs1004763, would not ($p=3.41\times10^{-8}$). Therefore, the relevance of rs1004763 to cortical thickness should be considered provisional until replicated.

The present gSEM was based on the GWAS results of Grasby et al¹⁸., which averaged left and right hemisphere phenotypic measures. This precluded an investigation of hemispheric asymmetries.

4.2 Conclusion

We harnessed the pervasive pleiotropy of the human cortex to realize a unique genetically-informed parcellation that is neurobiologically distinct from anatomical, functional, cytoarchitectural, and other established cortical parcellations, yet harbors meaningful topographic similarities to other network schemas, particularly resting-state fMRI networks. Strong genetic correlation between GIBNs and several major neuropsychiatric conditions including OCD, Bipolar, ADHD, and Alcohol Dependence, coupled with clear confirmation that nearly all GIBN-related SNPs play a role in cognitive, behavioral, neuroanatomical, and neurofunctional phenotypes, begins to expose the deeply interconnected architecture of the human cortex. Applying gSEM to model the joint genetic architecture of complex traits and investigate multivariate genetic links across phenotypes offers a new vantage point for mapping genetically informed cortical networks.

SUPPORT

National Institute for Mental Health Grant No. R01-MH111671, R01-MH129832, and VISN6 MIRECC (to RAM); VA Merit Grant Nos. 1I01RX000389-01 (to RAM) and 1I01CX000748-01A1 (to RAM); National Institute of Neurological Disorders and Stroke Grant Nos. 5R01NS086885-02 and K23 MH073091-01 (to RAM); National Health and Medical Research Council APP1173025 (to KLG). VA Career Development Award #1IK2CX002107 - US Department of Veterans Affairs CSR&D. ENIGMA was supported partly by NIH U54 EB020403 from the Big Data to Knowledge (BD2K) program, R56AG058854, R01MH116147, R01MH111671, and P41 EB015922 (to PMT); NIMH R01MH106595 (to CMN). We thank Cohen Veterans Bioscience for ongoing support and building a collaborative scientific environment.

We thank all members of the respective site laboratories within the ENIGMA who contributed to general study organization, recruitment, data collection, and management, as well as subsequent analyses. Most importantly, we thank all of our study participants for their efforts to take part in this study. The funding agencies had no part in the analysis of data or approval of the final publication. The views expressed in this article are those of the authors and do not necessarily reflect the position or policy of the Department of Veterans Affairs or the US government.

CONFLICTS OF INTEREST

Dr. Thompson received partial research support from Biogen, Inc. (Boston, USA) for research unrelated to the topic of this manuscript. No other authors have competing financial interests in relation to the research presented herein. The material presented is original research that has not been previously published and has not been submitted for publication elsewhere.

REFERENCES

1. Zielinski, B.A., Gennatas, E.D., Zhou, J., and Seeley, W.W. (2010). Network-level structural covariance in the developing brain. *Proceedings of the National Academy of Sciences* *107*, 18191-18196.
2. Romero-Garcia, R., Whitaker, K.J., Váša, F., Seidlitz, J., Shinn, M., Fonagy, P., Dolan, R.J., Jones, P.B., Goodyer, I.M., and Bullmore, E.T. (2018). Structural covariance networks are coupled to expression of genes enriched in supragranular layers of the human cortex. *Neuroimage* *171*, 256-267.
3. Feng, J., Chen, C., Cai, Y., Ye, Z., Feng, K., Liu, J., Zhang, L., Yang, Q., Li, A., and Sheng, J. (2020). Partitioning heritability analyses unveil the genetic architecture of human brain multidimensional functional connectivity patterns. *Human brain mapping* *41*, 3305-3317.
4. Hawrylycz, M., Miller, J.A., Menon, V., Feng, D., Dolbeare, T., Guillozet-Bongaarts, A.L., Jegga, A.G., Aronow, B.J., Lee, C.-K., and Bernard, A. (2015). Canonical genetic signatures of the adult human brain. *Nature neuroscience* *18*, 1832-1844.
5. Gong, G., He, Y., Chen, Z.J., and Evans, A.C. (2012). Convergence and divergence of thickness correlations with diffusion connections across the human cerebral cortex. *Neuroimage* *59*, 1239-1248.
6. Alexander-Bloch, A., Giedd, J.N., and Bullmore, E. (2013). Imaging structural co-variance between human brain regions. *Nature Reviews Neuroscience* *14*, 322-336.
7. Seeley, W.W., Crawford, R.K., Zhou, J., Miller, B.L., and Greicius, M.D. (2009). Neurodegenerative diseases target large-scale human brain networks. *Neuron* *62*, 42-52.
8. He, Y., Chen, Z., and Evans, A. (2008). Structural insights into aberrant topological patterns of large-scale cortical networks in Alzheimer's disease. *Journal of Neuroscience* *28*, 4756-4766.
9. Segall, J.M., Allen, E.A., Jung, R.E., Erhardt, E.B., Arja, S.K., Kiehl, K.A., and Calhoun, V.D. (2012). Correspondence between structure and function in the human brain at rest. *Frontiers in neuroinformatics* *6*, 10.
10. Zhang, Z., Liao, W., Zuo, X.-N., Wang, Z., Yuan, C., Jiao, Q., Chen, H., Biswal, B.B., Lu, G., and Liu, Y. (2011). Resting-state brain organization revealed by functional covariance networks. *PLoS One* *6*, e28817.
11. Chen, C.-H., Gutierrez, E., Thompson, W., Panizzon, M.S., Jernigan, T.L., Eyler, L.T., Fennema-Notestine, C., Jak, A.J., Neale, M.C., and Franz, C.E. (2012). Hierarchical genetic organization of human cortical surface area. *Science* *335*, 1634-1636.
12. Lenroot, R.K., Schmitt, J.E., Ordaz, S.J., Wallace, G.L., Neale, M.C., Lerch, J.P., Kendler, K.S., Evans, A.C., and Giedd, J.N. (2009). Differences in genetic and environmental influences on the human cerebral cortex associated with development during childhood and adolescence. *Human brain mapping* *30*, 163-174.
13. Schmitt, J., Lenroot, R., Wallace, G., Ordaz, S., Taylor, K., Kabani, N., Greenstein, D., Lerch, J., Kendler, K., and Neale, M. (2008). Identification of genetically mediated cortical networks: a multivariate study of pediatric twins and siblings. *Cerebral cortex* *18*, 1737-1747.
14. van der Meer, D., Frei, O., Kaufmann, T., Chen, C.-H., Thompson, W.K., O'Connell, K.S., Monereo Sánchez, J., Linden, D.E., Westlye, L.T., and Dale, A.M. (2020). Quantifying the polygenic architecture of the human cerebral cortex: extensive genetic overlap between cortical thickness and surface area. *Cerebral Cortex* *30*, 5597-5603.

15. Tichenor, M., and Sridhar, D. (2019). Metric partnerships: global burden of disease estimates within the World Bank, the World Health Organisation and the Institute for Health Metrics and Evaluation. *Wellcome Open Research* 4.
16. Rowland, T.A., and Marwaha, S. (2018). Epidemiology and risk factors for bipolar disorder. *Therapeutic advances in psychopharmacology* 8, 251-269.
17. Smith, S.M., Douaud, G., Chen, W., Hanayik, T., Alfaro-Almagro, F., Sharp, K., and Elliott, L.T. (2021). An expanded set of genome-wide association studies of brain imaging phenotypes in UK Biobank. *Nature neuroscience* 24, 737-745.
18. Grasby, K.L., Jahanshad, N., Painter, J.N., Colodro-Conde, L., Bralten, J., Hibar, D.P., Lind, P.A., Pizzagalli, F., Ching, C.R., and McMahon, M.A.B. (2020). The genetic architecture of the human cerebral cortex. *Science* 367.
19. Grotzinger, A.D., Rehmtulla, M., de Vlaming, R., Ritchie, S.J., Mallard, T.T., Hill, W.D., Ip, H.F., Marioni, R.E., McIntosh, A.M., and Deary, I.J. (2019). Genomic structural equation modelling provides insights into the multivariate genetic architecture of complex traits. *Nature human behaviour* 3, 513-525.
20. Kovas, Y., and Plomin, R. (2006). Generalist genes: implications for the cognitive sciences. *Trends in cognitive sciences* 10, 198-203.
21. Desikan, R.S., Ségonne, F., Fischl, B., Quinn, B.T., Dickerson, B.C., Blacker, D., Buckner, R.L., Dale, A.M., Maguire, R.P., and Hyman, B.T. (2006). An automated labeling system for subdividing the human cerebral cortex on MRI scans into gyral based regions of interest. *Neuroimage* 31, 968-980.
22. Grotzinger, A.D., Rehmtulla, M., de Vlaming, R., Ritchie, S.J., Mallard, T.T., Hill, W.D., Ip, H.F., Marioni, R.E., McIntosh, A.M., Deary, I.J., et al. (2019). Genomic structural equation modelling provides insights into the multivariate genetic architecture of complex traits. *Nat Hum Behav* 3, 513-525. 10.1038/s41562-019-0566-x.
23. de Vries, A., Tiemens, B., Cillessen, L., and Hutschemaekers, G. (2021). Construction and validation of a self-direction measure for mental health care. *J Clin Psychol* 77, 1371-1383. 10.1002/jclp.23091.
24. Watanabe, K., Taskesen, E., Van Bochoven, A., and Posthuma, D. (2017). Functional mapping and annotation of genetic associations with FUMA. *Nature communications* 8, 1-11.
25. 1000 Genomes Project Consortium, Auton, A., Brooks, L.D., Durbin, R.M., Garrison, E.P., Kang, H.M., Korbel, J.O., Marchini, J.L., McCarthy, S., McVean, G.A., and Abecasis, G.R. (2015). A global reference for human genetic variation. *Nature* 526, 68-74. 10.1038/nature15393.
26. Shadrin, A.A., Kaufmann, T., van der Meer, D., Palmer, C.E., Makowski, C., Loughnan, R., Jernigan, T.L., Seibert, T.M., Hagler, D.J., and Smeland, O.B. (2021). Vertex-wise multivariate genome-wide association study identifies 780 unique genetic loci associated with cortical morphology. *NeuroImage* 244, 118603.
27. Hofer, E., Roshchupkin, G.V., Adams, H.H., Knol, M.J., Lin, H., Li, S., Zare, H., Ahmad, S., Armstrong, N.J., and Satizabal, C.L. (2020). Genetic correlations and genome-wide associations of cortical structure in general population samples of 22,824 adults. *Nature communications* 11, 1-16.
28. Adams, H.H., Hibar, D.P., Chouraki, V., Stein, J.L., Nyquist, P.A., Rentería, M.E., Trompet, S., Arias-Vasquez, A., Seshadri, S., and Desrivière, S. (2016). Novel genetic loci underlying human intracranial volume identified through genome-wide association. *Nature neuroscience* 19, 1569-1582.

29. Elliott, L.T., Sharp, K., Alfaro-Almagro, F., Shi, S., Miller, K.L., Douaud, G., Marchini, J., and Smith, S.M. (2018). Genome-wide association studies of brain imaging phenotypes in UK Biobank. *Nature* **562**, 210-216.
30. Arfan Ikram, M., Fornage, M., Smith, A.V., Seshadri, S., Schmidt, R., Debette, S., Vrooman, H.A., Sigurdsson, S., Ropele, S., and Taal, H.R. (2012). Common variants at 6q22 and 17q21 are associated with intracranial volume. *Nature genetics* **44**, 539-544.
31. Hibar, D.P., Stein, J.L., Renteria, M.E., Arias-Vasquez, A., Desrivieres, S., Jahanshad, N., Toro, R., Wittfeld, K., Abramovic, L., Andersson, M., et al. (2015). Common genetic variants influence human subcortical brain structures. *Nature*. [10.1038/nature14101](https://doi.org/10.1038/nature14101).
32. Demontis, D., Walters, R.K., Martin, J., Mattheisen, M., Als, T.D., Agerbo, E., Baldursson, G., Belliveau, R., Bybjerg-Grauholm, J., and Bækvad-Hansen, M. (2019). Discovery of the first genome-wide significant risk loci for attention deficit/hyperactivity disorder. *Nature genetics* **51**, 63.
33. Walters, R.K., Polimanti, R., Johnson, E.C., McClintick, J.N., Adams, M.J., Adkins, A.E., Aliev, F., Bacanu, S.-A., Batzler, A., and Bertelsen, S. (2018). Transancestral GWAS of alcohol dependence reveals common genetic underpinnings with psychiatric disorders. *Nature neuroscience* **21**, 1656-1669.
34. Watson, H.J., Yilmaz, Z., Thornton, L.M., Hübel, C., Coleman, J.R., Gaspar, H.A., Bryois, J., Hinney, A., Leppä, V.M., and Mattheisen, M. (2019). Genome-wide association study identifies eight risk loci and implicates metabo-psychiatric origins for anorexia nervosa. *Nature genetics* **51**, 1207-1214.
35. Grove, J., Ripke, S., Als, T.D., Mattheisen, M., Walters, R.K., Won, H., Pallesen, J., Agerbo, E., Andreassen, O.A., and Anney, R. (2019). Identification of common genetic risk variants for autism spectrum disorder. *Nature genetics* **51**, 431-444.
36. Stahl, E.A., Breen, G., Forstner, A.J., McQuillin, A., Ripke, S., Trubetskoy, V., Mattheisen, M., Wang, Y., Coleman, J.R., and Gaspar, H.A. (2019). Genome-wide association study identifies 30 loci associated with bipolar disorder. *Nature genetics* **51**, 793-803.
37. Johnson, E.C., Demontis, D., Thorgeirsson, T.E., Walters, R.K., Polimanti, R., Hatoum, A.S., Sanchez-Roige, S., Paul, S.E., Wendt, F.R., and Clarke, T.-K. (2020). A large-scale genome-wide association study meta-analysis of cannabis use disorder. *The Lancet Psychiatry* **7**, 1032-1045.
38. Howard, D.M., Adams, M.J., Clarke, T.-K., Hafferty, J.D., Gibson, J., Shirali, M., Coleman, J.R., Hagenaars, S.P., Ward, J., and Wigmore, E.M. (2019). Genome-wide meta-analysis of depression identifies 102 independent variants and highlights the importance of the prefrontal brain regions. *Nature neuroscience* **22**, 343-352.
39. Arnold, P.D., Askland, K.D., Barlassina, C., Bellodi, L., Bienvenu, O., Black, D., Bloch, M., Brentani, H., Burton, C.L., and Camarena, B. (2018). Revealing the complex genetic architecture of obsessive-compulsive disorder using meta-analysis. *Molecular psychiatry* **23**, 1181-1181.
40. Maihofer, A.X., Choi, K.W., Coleman, J.R., Daskalakis, N.P., Denckla, C.A., Ketema, E., Morey, R.A., Polimanti, R., Ratanatharathorn, A., and Torres, K. (2021). Enhancing Discovery of Genetic Variants for Posttraumatic Stress Disorder Through Integration of Quantitative Phenotypes and Trauma Exposure Information. *Biological psychiatry*.

41. Trubetskoy, V., Pardiñas, A.F., Qi, T., Panagiotaropoulou, G., Awasthi, S., Bigdeli, T.B., Bryois, J., Chen, C.-Y., Dennison, C.A., and Hall, L.S. (2022). Mapping genomic loci implicates genes and synaptic biology in schizophrenia. *Nature* *604*, 502-508.
42. Yu, D., Sul, J.H., Tsetsos, F., Nawaz, M.S., Huang, A.Y., Zelaya, I., Illmann, C., Osiecki, L., Darrow, S.M., and Hirschtritt, M.E. (2019). Interrogating the genetic determinants of Tourette's syndrome and other tic disorders through genome-wide association studies. *American Journal of Psychiatry* *176*, 217-227.
43. Otowa, T., Hek, K., Lee, M., Byrne, E.M., Mirza, S.S., Nivard, M.G., Bigdeli, T., Aggen, S.H., Adkins, D., and Wolen, A. (2016). Meta-analysis of genome-wide association studies of anxiety disorders. *Molecular psychiatry* *21*, 1391-1399.
44. Bulik-Sullivan, B.K., Loh, P.-R., Finucane, H.K., Ripke, S., Yang, J., Patterson, N., Daly, M.J., Price, A.L., Neale, B.M., and Consortium, S.W.G.o.t.P.G. (2015). LD Score regression distinguishes confounding from polygenicity in genome-wide association studies. *Nature genetics* *47*, 291-295.
45. Wolfe, D., Dudek, S., Ritchie, M.D., and Pendergrass, S.A. (2013). Visualizing genomic information across chromosomes with PhenoGram. *BioData mining* *6*, 1-12.
46. van der Meer, D., Frei, O., Kaufmann, T., Shadrin, A.A., Devor, A., Smeland, O.B., Thompson, W.K., Fan, C.C., Holland, D., and Westlye, L.T. (2020). Understanding the genetic determinants of the brain with MOSTest. *Nature communications* *11*, 1-9.
47. Zhao, B., Li, T., Yang, Y., Wang, X., Luo, T., Shan, Y., Zhu, Z., Xiong, D., Hauberg, M.E., and Bendl, J. (2021). Common genetic variation influencing human white matter microstructure. *Science* *372*, eabf3736.
48. Zhao, B., Luo, T., Li, T., Li, Y., Zhang, J., Shan, Y., Wang, X., Yang, L., Zhou, F., and Zhu, Z. (2019). Genome-wide association analysis of 19,629 individuals identifies variants influencing regional brain volumes and refines their genetic co-architecture with cognitive and mental health traits. *Nature genetics* *51*, 1637-1644.
49. Donati, G., Dumontheil, I., Pain, O., Asbury, K., and Meaburn, E.L. (2021). Evidence for specificity of polygenic contributions to attainment in English, maths and science during adolescence. *Scientific reports* *11*, 1-11.
50. Lee, J.J., Wedow, R., Okbay, A., Kong, E., Maghzian, O., Zacher, M., Nguyen-Viet, T.A., Bowers, P., Sidorenko, J., and Karlsson Linnér, R. (2018). Gene discovery and polygenic prediction from a genome-wide association study of educational attainment in 1.1 million individuals. *Nature genetics* *50*, 1112-1121.
51. Savage, J.E., Jansen, P.R., Stringer, S., Watanabe, K., Bryois, J., De Leeuw, C.A., Nagel, M., Awasthi, S., Barr, P.B., and Coleman, J.R. (2018). Genome-wide association meta-analysis in 269,867 individuals identifies new genetic and functional links to intelligence. *Nature genetics* *50*, 912-919.
52. Hill, W.D., Marioni, R.E., Maghzian, O., Ritchie, S.J., Hagenaars, S.P., McIntosh, A., Gale, C.R., Davies, G., and Deary, I.J. (2019). A combined analysis of genetically correlated traits identifies 187 loci and a role for neurogenesis and myelination in intelligence. *Molecular psychiatry* *24*, 169-181.
53. Demange, P.A., Malanchini, M., Mallard, T.T., Biroli, P., Cox, S.R., Grotzinger, A.D., Tucker-Drob, E.M., Abdellaoui, A., Arseneault, L., and Van Bergen, E. (2021). Investigating the genetic architecture of noncognitive skills using GWAS-by-subtraction. *Nature genetics* *53*, 35-44.

54. Davies, G., Lam, M., Harris, S.E., Trampush, J.W., Luciano, M., Hill, W.D., Hagenaars, S.P., Ritchie, S.J., Marioni, R.E., and Fawns-Ritchie, C. (2018). Study of 300,486 individuals identifies 148 independent genetic loci influencing general cognitive function. *Nature communications* 9, 1-16.
55. Ge, T., Chen, C.Y., Doyle, A.E., Vettermann, R., Tuominen, L.J., Holt, D.J., Sabuncu, M.R., and Smoller, J.W. (2019). The Shared Genetic Basis of Educational Attainment and Cerebral Cortical Morphology. *Cereb Cortex* 29, 3471-3481. 10.1093/cercor/bhy216.
56. Linnér, K., Biroli, P., Kong, E., Meddents, S.F.W., Wedow, R., Fontana, M.A., Lebreton, M., Tino, S.P., Abdellaoui, A., and Hammerschlag, A.R. (2019). Genome-wide association analyses of risk tolerance and risky behaviors in over 1 million individuals identify hundreds of loci and shared genetic influences. *Nature genetics* 51, 245-257.
57. Karlsson Linner, R., Biroli, P., Kong, E., Meddents, S.F.W., Wedow, R., Fontana, M.A., Lebreton, M., Tino, S.P., Abdellaoui, A., Hammerschlag, A.R., et al. (2019). Genome-wide association analyses of risk tolerance and risky behaviors in over 1 million individuals identify hundreds of loci and shared genetic influences. *Nat Genet* 51, 245-257. 10.1038/s41588-018-0309-3.
58. Goes, F.S., McGrath, J., Avramopoulos, D., Wolyniec, P., Pirooznia, M., Ruczinski, I., Nestadt, G., Kenny, E.E., Vacic, V., and Peters, I. (2015). Genome-wide association study of schizophrenia in Ashkenazi Jews. *American Journal of Medical Genetics Part B: Neuropsychiatric Genetics* 168, 649-659.
59. Lam, M., Chen, C.-Y., Li, Z., Martin, A.R., Bryois, J., Ma, X., Gaspar, H., Ikeda, M., Benyamin, B., and Brown, B.C. (2019). Comparative genetic architectures of schizophrenia in East Asian and European populations. *Nature genetics* 51, 1670-1678.
60. Pardiñas, A.F., Holmans, P., Pocklington, A.J., Escott-Price, V., Ripke, S., Carrera, N., Legge, S.E., Bishop, S., Cameron, D., and Hamshere, M.L. (2018). Common schizophrenia alleles are enriched in mutation-intolerant genes and in regions under strong background selection. *Nature genetics* 50, 381-389.
61. Sullivan, P.F., Agrawal, A., Bulik, C.M., Andreassen, O.A., Børglum, A.D., Breen, G., Cichon, S., Edenberg, H.J., Faraone, S.V., and Gelernter, J. (2018). Psychiatric genomics: an update and an agenda. *American Journal of Psychiatry* 175, 15-27.
62. Wu, Y., Cao, H., Baranova, A., Huang, H., Li, S., Cai, L., Rao, S., Dai, M., Xie, M., and Dou, Y. (2020). Multi-trait analysis for genome-wide association study of five psychiatric disorders. *Translational psychiatry* 10, 1-11.
63. Yao, X., Glessner, J.T., Li, J., Qi, X., Hou, X., Zhu, C., Li, X., March, M.E., Yang, L., and Mentch, F.D. (2021). Integrative analysis of genome-wide association studies identifies novel loci associated with neuropsychiatric disorders. *Translational psychiatry* 11, 1-12.
64. Smeland, O.B., Shadrin, A., Bahrami, S., Broce, I., Tesli, M., Frei, O., Wirgenes, K.V., O'Connell, K.S., Krull, F., and Bettella, F. (2021). Genome-wide association analysis of Parkinson's disease and schizophrenia reveals shared genetic architecture and identifies novel risk loci. *Biological psychiatry* 89, 227-235.
65. Pickrell, J.K., Berisa, T., Liu, J.Z., Ségurel, L., Tung, J.Y., and Hinds, D.A. (2016). Detection and interpretation of shared genetic influences on 42 human traits. *Nature genetics* 48, 709-717.
66. van de Vegte, Y.J., Said, M.A., Rienstra, M., van der Harst, P., and Verweij, N. (2020). Genome-wide association studies and Mendelian randomization analyses for leisure sedentary behaviours. *Nature communications* 11, 1-10.

67. de la Fuente, J., Davies, G., Grotzinger, A.D., Tucker-Drob, E.M., and Deary, I.J. (2021). A general dimension of genetic sharing across diverse cognitive traits inferred from molecular data. *Nature Human Behaviour* 5, 49-58.
68. Takayanagi, Y., Sasabayashi, D., Takahashi, T., Furuichi, A., Kido, M., Nishikawa, Y., Nakamura, M., Noguchi, K., and Suzuki, M. (2020). Reduced Cortical Thickness in Schizophrenia and Schizotypal Disorder. *Schizophr Bull* 46, 387-394. 10.1093/schbul/sbz051.
69. Siddarth, P., Burggren, A.C., Eyre, H.A., Small, G.W., and Merrill, D.A. (2018). Sedentary behavior associated with reduced medial temporal lobe thickness in middle-aged and older adults. *PLoS One* 13, e0195549. 10.1371/journal.pone.0195549.
70. Richiardi, J., Altmann, A., Milazzo, A.-C., Chang, C., Chakravarty, M.M., Banaschewski, T., Barker, G.J., Bokde, A.L., Bromberg, U., and Büchel, C. (2015). Correlated gene expression supports synchronous activity in brain networks. *Science* 348, 1241-1244.
71. Noble, S., Scheinost, D., and Constable, R.T. (2019). A decade of test-retest reliability of functional connectivity: A systematic review and meta-analysis. *Neuroimage* 203, 116157.
72. Damoiseaux, J.S., Rombouts, S., Barkhof, F., Scheltens, P., Stam, C.J., Smith, S.M., and Beckmann, C.F. (2006). Consistent resting-state networks across healthy subjects. *Proceedings of the national academy of sciences* 103, 13848-13853.
73. Yeo, B.T.T., Krienen, F.M., Sepulcre, J., Sabuncu, M.R., Lashkari, D., Hollinshead, M., Roffman, J.L., Smoller, J.W., Zoller, L., Polimeni, J.R., et al. (2011). The organization of the human cerebral cortex estimated by intrinsic functional connectivity. *Journal of Neurophysiology* 106, 1125-1165. DOI 10.1152/jn.00338.2011.
74. Anderson, K.M., Ge, T., Kong, R., Patrick, L.M., Spreng, R.N., Sabuncu, M.R., Yeo, B.T., and Holmes, A.J. (2021). Heritability of individualized cortical network topography. *Proceedings of the National Academy of Sciences* 118.
75. Forseth, K.J., Hickok, G., Rollo, P., and Tandon, N. (2020). Language prediction mechanisms in human auditory cortex. *Nature communications* 11, 1-14.
76. Celesia, G.G. (1976). Organization of auditory cortical areas in man. *Brain* 99, 403-414.
77. Mengotti, P., Käsbauer, A.-S., Fink, G.R., and Vossel, S. (2020). Lateralization, functional specialization, and dysfunction of attentional networks. *Cortex* 132, 206-222.
78. Lee, S., Parthasarathi, T., and Kable, J.W. (2021). The ventral and dorsal default mode networks are dissociably modulated by the vividness and valence of imagined events. *Journal of Neuroscience* 41, 5243-5250.
79. Greene, C.M., and Soto, D. (2014). Functional connectivity between ventral and dorsal frontoparietal networks underlies stimulus-driven and working memory-driven sources of visual distraction. *NeuroImage* 84, 290-298.
80. Fu, Y., Ma, Z., Hamilton, C., Liang, Z., Hou, X., Ma, X., Hu, X., He, Q., Deng, W., and Wang, Y. (2015). Genetic influences on resting-state functional networks: A twin study. *Human brain mapping* 36, 3959-3972.
81. Munji, R.N., Choe, Y., Li, G., Siegenthaler, J.A., and Pleasure, S.J. (2011). Wnt signaling regulates neuronal differentiation of cortical intermediate progenitors. *Journal of Neuroscience* 31, 1676-1687.
82. Rakic, P. (2009). Evolution of the neocortex: a perspective from developmental biology. *Nature Reviews Neuroscience* 10, 724-735.

83. Polimanti, R., Ratanatharathorn, A., Maihofer, A.X., Choi, K.W., Stein, M.B., Morey, R.A., Logue, M.W., Nievergelt, C.M., Stein, D.J., and Koenen, K.C. (2019). Association of economic status and educational attainment with posttraumatic stress disorder: a Mendelian randomization study. *JAMA network open* 2, e193447-e193447.